2013 European Control Conference (ECC)
July 17-19, 2013, Zürich, Switzerland.

Robust Attitude Control for an Unmanned Helicopter in near-hover flights

Panos Marantos, Leonidas Dritsas and Kostas J. Kyriakopoulos

Abstract— **In this paper, a systematic procedure for designing robust attitude controllers for unmanned helicopters, based on mixed H_2/H_∞ methodologies, is presented. Firstly, a family of linearized models describing the near-hover flight dynamics is derived which can be compactly formulated as a nominal plant perturbed by norm bound uncertainties on the system, control and wind matrices. It is then shown that a single robust controller can be designed guaranteeing stability, robustness and gust disturbance rejection for the whole near-hover flight envelope. Performance analysis and simulation results show that the proposed attitude control strategy can also satisfy the handling qualities defined in ADS-33E specification requirements. Finally, the attitude controller is used as a module in a total control scheme offering position tracking capabilities which is implemented in a real embedded system. The efficacy of the total control structure is proved by Hardware-In-the-Loop simulations on an accurate nonlinear helicopter model.**

I. INTRODUCTION

The research community has shown a growing interest in Unmanned Air Helicopters (UAH), due to their applicability in dynamic and unknown environments. Major applications of UAHs are search and rescue, surveillance and remote inspection [1]. The capabilities of hovering, vertical takeoff/landing (VTOL), autorotationing, taking off(landing) from(to) every desired area and their high maneuverability (pirouette and slalom) make helicopters an attractive choice.

However, those advantages come at the expense of a rather complicated autopilot. The combination of (i) multivariable nonlinear dynamics, (ii) couplings between all states, (iii) rotor dynamics and aerodynamics that can not be directly measured or easily estimated (iv) the presence of wind disturbances and (v) uncertainties in aerodynamic coefficients, complicate the control design procedure. Moreover helicopters are underactuated systems since the available control input signals are fewer than the degrees of freedom to be controlled. This makes common inverse-dynamics approaches or feedback linearization techniques inapplicable. Thus UAHs constitute an interesting and difficult testbed for the design of sophisticated control algorithms.

Several approaches have been proposed using either nonlinear techniques, usually based on low order/simplified nonlinear helicopter models [2][3][4], or linear techniques due to the easiness of implementation on common embedded systems [5][6].

Nevertheless, various H_∞ approaches for the design of UAH controllers have been reported and implemented. See for example [7] and the references therein. The authors in [1] proposed the design of two robust dynamic controllers to track a predefined trajectory and handle exogenous disturbances (wind) that occur through flight. Similarly the authors in [8] proposed the design of two controllers combining H_∞ loop shaping and static output feedback techniques that can produce reduced order controllers. In all these approaches, the system is decomposed in order to design separate controllers for attitude stabilization and position trajectory tracking. Along the same lines, in [9], state feedback techniques and H_∞ are combined.

The aerospace industry on the other hand has adopted handling qualities specification standards (ADS-33E) which can be used as performance design guidelines [10]. In ADS-33E, a number of command response-types are defined. We focus on Attitude Command Attitude Holding (ACAH) which is properly quantified so that it can be used as an experimental "a posteriori" performance evaluator.

Our aim in this work is to design and implement a single robust attitude stabilizing controller for a variety of near hover flight modes, based on mixed H_2/H_∞ concepts [11],[12],[13],[14]. Apart from stability, various performance specifications such as reference tracking, rejection of wind gust disturbances, actuators constraints and robustness to modeling uncertainties can be handled by a single controller designed via the proposed approach.

The first step is to linearize the nonlinear model around several trim points for a certain range of velocities near hover. Using interval arithmetics [15], this set of linearized plants can be formulated as a nominal linear plant with norm bounded uncertainties (NBU) that is used for the control design [9]. The next step is to formulate all three design (performance) objectives as H_2 or H_∞ optimization problems expressed as a set of Linear Matrix Inequalities (LMI). If this set of LMIs is feasible, a dynamic output feedback controller (DynOF) is derived and tested against a set of ADS-33E requirements.

Finally, a reduced order controller with tracking capabilities is designed based on a combination of loop shaping and static output feedback control methods [8]. This total position tracker is discretized, implemented in a modern embedded system and tested over a hardware-in-the-loop (HIL) testbed which uses the accurate fully nonlinear dynamics of a small-sized helicopter.

The paper is organized as follows: Section II presents the nonlinear helicopter model used for linearization and simulation along with the necessary steps leading to a nominal linear system perturbed by norm bound uncertainties. The

Authors are with the Control System Lab, Department of Electrical Engineering, School of Mechanical Engineering, National Technical University of Athens, Greece. marantos@mail.ntua.gr, ldri@otenet.gr, kkyria@mail.ntua.gr

systematic methodology of designing the proposed attitude controller is illustrated in Section III. Performance analysis is shown in Section IV. In Section V the total position tracking controller is presented along with the HIL implementation. Conclusion remarks and future plans are given in Section VI.

The notation $\text{diag}[X_1,\ldots,X_n]$ signifies a diagonal matrix with matrices $X_1,\ldots,X_n$ on the diagonal, while I_n is the $n\times n$ identity matrix.

II. SYSTEM MODELLING

A. Nonlinear Model

The well studied 6-DOF nonlinear model of a miniature helicopter given in [1] is enhanced with servo dynamics, swashplate kinematics and additional flapping derivatives due to translational velocities based on [2] to provide a complete model for this research. The benefit coming from this added complexity is the improved understanding of the helicopter response, gained via extensive simulations. This is an important first step before the actual experimental implementation.

The UAH is modeled as a 6-DOF rigid-body using Newton-Euler equations:

$$\begin{aligned}\dot{V}_b &= -\omega_b \times V_b + F_b/m \\ \dot{\omega}_b &= J^{-1}\left(M_b - \omega_b \times J\omega_b\right)\end{aligned} \tag{1}$$

where, $V_b = [\ u_b\ v_b\ w_b\ ]^T$ are the translational velocities in body frame (Fig.1), $\omega_b = [\ p\ q\ r\ ]^T$ are the rotational velocities, m is the helicopter mass, J is a diagonal matrix of moments of inertia in each axis, while F_b and M_b represent the total vectors of forces and moments acting on body frame, respectively. The differential kinematics equations are:

$$\begin{aligned}\dot{P}_e &= R(\Phi)\dot{P}_n = R(\Phi)V_b \\ \dot{\Phi} &= S^{-1}(\Phi)\omega_b\end{aligned} \tag{2}$$

where $P_e = [\ x_e\ y_e\ z_e\ ]^T$ is the vector of helicopter position in the inertial frame, $\dot{P}_n = [\ \dot{x}_n\ \dot{y}_n\ \dot{z}_n\ ]^T = V_b$, $\Phi = [\ \phi\ \theta\ \psi\ ]^T$ are euler angles and $R(\Phi)$ and $S(\Phi)$ are the rotational and lumped transformation matrices, respectively[6]. Note that for the computation of forces (F_b) and moments (M_b) the wind effects are taken into account [1].

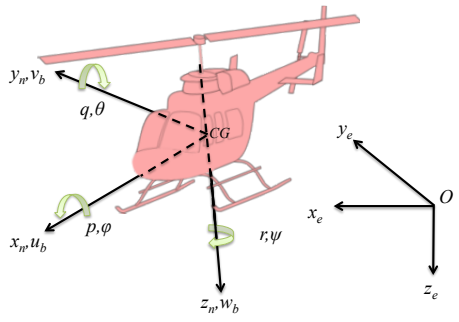

Fig. 1. Helicopter states

To complete the model we need to introduce the longitudinal and lateral flapping angles a_s, b_s, the intermediate state r_{fb} of the embedded yaw controller, the intermediate states of main and tail servo dynamics $s_0^*, s_1^*, s_2^*, s_{tail}^*$, the angles of the three servos s_0, s_1, s_2, the yaw rate command s_r and the main rotor speed command s_Ω. The range of the two last signals is normalized to (-1,1) and (0,1) respectively.

Combining (1),(2) the full nonlinear Helicopter model, writes as:

$$\begin{aligned}\dot{x}_f &= f_f(x_f, u_f) \\ x_f &= [\ x_e\ y_e\ z_e\ u_b\ v_b\ w_b\ p\ q\ r\ \phi\ \theta\ \psi\ a_s\ b_s\ r_{fb}\ s_0^*\ s_1^*\ s_2^*\ s_{tail}^*\ ]^T \\ u_f &= [\ s_0\ s_1\ s_2\ s_r\ s_\Omega\ ]^T\end{aligned} \tag{3}$$

B. Linear modeling via interval arithmetics

The linearization of system (3) pre-assumes some realistic simplifying assumptions, common in the relevant literature, which are: (i) the servo dynamics is neglected, (ii) the main rotor speed is constant through the flight and (iii) thera are exists a linear relationship between main servos and collective (δ_{col}), longitudinal (δ_{lon}) and lateral (δ_{lat}) pitch angles of the main rotor ($\delta = [\ \delta_{col}\ \delta_{lon}\ \delta_{lat}\ ]^T = K_s^\delta [\ s_0\ s_1\ s_2\ ]^T$). Therefore, the modified helicopter dynamics now becomes:

$$\begin{aligned}\dot{x} &= f(x,u) \\ x &= [\ x_n\ y_n\ z_n\ u_b\ v_b\ w_b\ p\ q\ r\ \phi\ \theta\ \psi\ a_s\ b_s\ r_{fb}\ ]^T \\ u &= [\ \delta_{col}\ \delta_{lon}\ \delta_{lat}\ s_r\ ]^T\end{aligned} \tag{4}$$

Noticing that in (4) the state vector x includes P_n rather than P_e, can proceed with linearization around a desired equilibrium. Thus, using the helicopter parameters appearing in [1] we formulate an extensive set of 462 different "pairs" of equilibrium states x_{eq} and equilibrium inputs u_{eq} each of which satisfies:

$$\dot{x} = 0 \bigcap \left|\sqrt{u_b^2 + v_b^2 + w_b^2}\right| \leq V_{air}^{nh}$$

where the maximum near hover airspeed velocity (V_{air}^{nh}) for this helicopter is equal to $2.38m/s$.

For all these trim points, using the analytic expressions of stability (system) derivatives, control derivatives and the elements of wind matrix, a family of linearized plants can be computed and represented in the form of an interval system [15]:

$$\begin{aligned}\dot{x} &= \mathbf{A}x + \mathbf{B}u + \mathbf{E}V_w \\ y &= Cx\end{aligned} \tag{5}$$

where $V_w = [\ u_w\ v_w\ w_w\ ]$ is the wind velocity vector acting on body frame and the interval matrices $\mathbf{A},\mathbf{B},\mathbf{E}$, satisfying the following elementwise inequalities (See [15] for definitions and notations):

$$\begin{aligned}\mathbf{A} &= \left[\underline{A},\bar{A}\right] = \left\{A;\underline{A} \leqslant A \leqslant \bar{A}\right\} \\ \mathbf{B} &= \left[\underline{B},\bar{B}\right] = \left\{B;\underline{B} \leqslant B \leqslant \bar{B}\right\} \\ \mathbf{E} &= \left[\underline{E},\bar{E}\right] = \left\{E;\underline{E} \leqslant E \leqslant \bar{E}\right\}\end{aligned} \tag{6}$$

Let us define the nominal ($_0$) system, control and wind matrices and their skew counterparts ($_{sk}$) as:

$$A_0 = \tfrac{1}{2}(\bar{A}+\underline{A}), \quad A_{sk} = \tfrac{1}{2}(\bar{A}-\underline{A})$$
$$B_0 = \tfrac{1}{2}(\bar{B}+\underline{B}), \quad B_{sk} = \tfrac{1}{2}(\bar{B}-\underline{B})$$
$$E_0 = \tfrac{1}{2}(\bar{E}+\underline{E}), \quad E_{sk} = \tfrac{1}{2}(\bar{E}-\underline{E})$$

Using standard interval arithmetics [15] [9],one can represent the interval system (5) as an norm bound uncertain (NBU) system in the form :

$$\begin{aligned} \dot{x} &= (A_0 + M_A\Delta_A N_A)x + (B_0 + M_B\Delta_B N_B)u + \\ &+ (E_0 + M_E\Delta_E N_E)V_w \\ y &= Cx \end{aligned} \tag{7}$$

where the pairs (M_A, N_A), (M_B, N_B) and (M_E, N_E) are derived from the skew matrices A_{sk}, B_{sk} and E_{sk} respectively, and Δ_A, Δ_B, Δ_E are diagonal uncertain matrices of appropriate dimensions whose elements satisfy $|\delta_{ii}| \leq 1$.

The resulting uncertain plant, reflecting the whole family of linearized plants for the selected range of different velocities, has the same state and input vector as the nonlinear model (4), while the standard output/measurement vector of the helicopter is:

$$y = [\ x_n\ y_n\ z_n\ u_b\ v_b\ w_b\ p\ q\ r\ \phi\ \theta\ \psi\ ]^T$$

III. Attitude Control Design

An essential step in the control design is the decomposition of the system into rotational (Inner) and translational (Outer) subsystems. This approach (typical in the UAV Helicopter literature [6], [1], [9]) helps to overcome the underactuation of the system and enables the setup of different performance specifications for each subsystem. This decomposition suggests an appropriate control structure as shown in Fig.2.

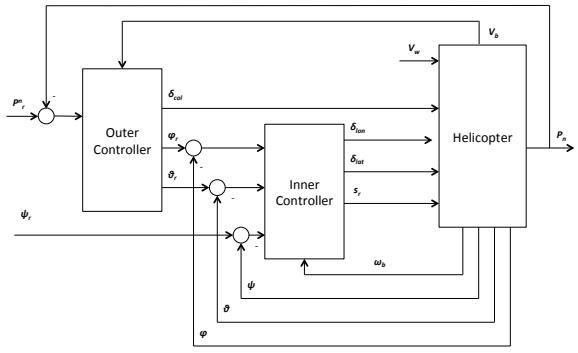

Fig. 2. Block Diagram of Composite Control Structure

A. Inner Subsystem

The decomposition of full order uncertain plant (7) into its inner and outer subsystems yields :

$$\begin{bmatrix} \dot{x}_{in} \\ \dot{x}_{out} \end{bmatrix} = \begin{bmatrix} A_{in} + M_A^{in}\Delta_A^{in}N_A^{in} & D_{out} \\ D_{in} & A_{out} + M_A^{out}\Delta_A^{out}N_A^{out} \end{bmatrix} \begin{bmatrix} x_{in} \\ x_{out} \end{bmatrix}$$
$$\ldots + \begin{bmatrix} B_{in} + M_B^{in}\Delta_B^{in}N_B^{in} & F_{out} \\ F_{in} & B_{out} + M_B^{out}\Delta_B^{out}N_B^{out} \end{bmatrix} \begin{bmatrix} u_{in} \\ u_{out} \end{bmatrix}$$
$$\ldots + \begin{bmatrix} E_{in} + M_E^{in}\Delta_E^{in}N_E^{in} \\ E_{out} + M_E^{out}\Delta_E^{out}N_E^{out} \end{bmatrix} [\ V_w\ ] \tag{8}$$

where, $x_{in} = [\ p\ q\ r\ \phi\ \theta\ \psi\ a_s\ b_s\ r_{fb}\ ]^T$ is the state vector of inner dynamics, $x_{out} = [\ x_n\ y_n\ z_n\ u_b\ v_b\ w_b\ ]^T$ is the state vector of outer dynamics and $u_{in} = [\ \delta_{lon}\ \delta_{lat}\ s_r\ ]^T$, $u_{out} = \delta_{col}$ are the corresponding input vectors.

Assuming that in (8) x_{out} and u_{out} act as constant unknown disturbances to be handled, the control design will be based on the following simplified inner attitude subsystem:

$$\begin{aligned} \dot{x}_{in} &= (A_{in} + M_A^{in}\Delta_A^{in}N_A^{in})x_{in} + (B_{in} + M_B^{in}\Delta_B^{in}N_B^{in})u_{in} + \\ &+ (E_{in} + M_E^{in}\Delta_E^{in}N_E^{in})V_w \\ y_c^i &= C_{in}^c x_{in}, \quad y_m^i = C_{in}^m x_{in} \end{aligned} \tag{9}$$

where $y_c^i = [\ \phi\ \theta\ \psi\ ]^T$ is the output to be controlled and $y_m^i = [\ p\ q\ r\ ]^T$ is a vector of additional output measurements and C_{in}^c, C_{in}^m are appropriate output matrices.

B. Mixed H_2/H_∞ Control Design

The mixed H_2/H_∞ approach provides a unifying framework for the design of a single dynamic output feedback controller which can simultaneously satisfy the design objectives of internal stability, reference tracking, disturbance rejection and uncertainty handling [12], [13].

All design objectives can be expressed as optimization problems on appropriately defined transfer functions in the generalized plant shown in Fig.3 . The input signals to the generalized plant are the reference trajectory $r(t)$, the wind velocities $V_w(t)$ and the perturbation signal w_Δ while z, z_Δ represent signals to be regulated. The W_1, W_2, W_3 weighting filters incorporate the designer's frequency domain demands on the closed-loop system. More specifically:

- $W_1(s)$ shapes the output sensitivity function and hence sets bounds on the tracking error $e = r - y_c$ while maintaining the effects of the exogenous disturbances below a certain bound. The signal r consists the three attitude commands ϕ_r, θ_r and ψ_r.
- $W_2(s)$ shapes the control signals so that they conform with actuators' constraints.
- $W_3(s)$ guards the system against unmodeled high-frequency dynamics and maximizes the robustness of the controller with respect to multiplicative model uncertainties.

The reference tracking objective will be expressed as a minimization of the H_2 norm of the transfer function T_{zr}. The wind disturbance rejection will be expressed as a minimization of the H_∞ norm of the transfer function T_{zV_w}, while the uncertainty handling (robustness) requirement can be expressed as a constraint on the H_∞ norm of the transfer function $T_{z_\Delta w_\Delta}$. Putting all these objectives together the design of mixed H_2/H_∞ procedure can be formulated as: among all internally stabilizing controllers $K(s)$ choose the one that:

$$\begin{aligned} &\text{minimizes } (\gamma_2 + \gamma_\infty) \\ &\text{subject to:} \\ &\|T_{zr}\|_2 \leq \gamma_2, \quad \|T_{zV_w}\|_\infty \leq \gamma_\infty, \quad \left\|T_{z_\Delta w_\Delta}\right\|_\infty \leq 1 \end{aligned} \tag{10}$$

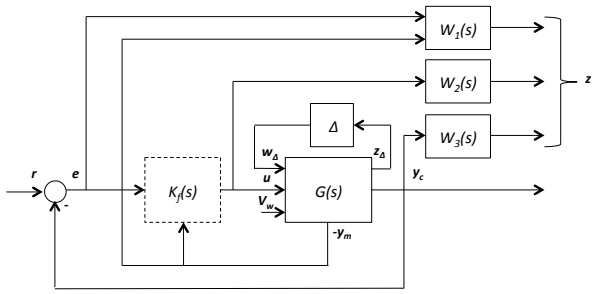

Fig. 3. Block Diagram of Closed-Loop Generalized Plant

The above multi-objective optimization can be cast into LMI formulation given in [16].

The NBU of the inner-subsystem (9) has to be transformed into an upper-LFT uncertainty block as shown in Fig.3. The inner subsystem now writes as:

$$\begin{aligned} \dot{x}_{in} &= A_{in}x_{in} + B_{in}u_{in} + E_{in}V_w + Mw_\Delta \\ y_c^i &= C_{in}^c x_{in}, \quad y_m^i = C_{in}^m x_{in} \\ z_\Delta &= N_x x_{in} + N_u u_{in} + N_w V_w \\ w_\Delta &= \Delta z_\Delta \end{aligned} \tag{11}$$

where

$$\begin{aligned} M = diag(M_A^{in}, M_B^{in}, M_E^{in}), \quad N_x = diag(N_A^{in}, O, O) \\ N_u = diag(O, N_B^{in}, O), \quad N_w = diag(O, O, N_E^{in}) \end{aligned}$$

and $\Delta = diag(\Delta_A^{in}, \Delta_B^{in}, \Delta_E^{in})$ where O zero matrices of appropriate dimensions.

C. Performance Specifications

The next crucial step in the attitude controller design is the selection of appropriate weighting functions that reflect the specifications below:

- The closed loop system can track step commands.
- The closed loop system must be robustly stable over the entire near hover flight envelope.
- The closed loop response has rise time less than 1sec, settling time less than 1.5sec , overshoot less than 5% and 0.1% steady-state error.
- The controller rejects 99% of exogenous disturbances.
- The control signal must respect the constrains of servo dynamics in order to avoid saturation.
- Comply with Level 1 requirements for ACAH mode.

As shown in Fig.3 the additional output measurements y_m^i are exploited by feeding them directly into the controller. The only demand made on these signals is that they are kept bounded. After few trials, the filter $W_1(s)$ is chosen as:

$$W_1 = diag\left[\tfrac{37s+0.137}{s+0.001}, \tfrac{72s+1.112}{6s+0.001}, \tfrac{30s+0.12}{1.5s+0.001}, 0.01, 0.01, 0.01\right]$$

In order to protect the servo actuators from saturation, the following selection is made: $W_2 = diag\,[1,\ 1,\ 1\ ]$, while $W_3 = diag\,[0.1,\ 0.1,\ 0.1]$.

It was also found practically necessary to constrain the closed-loop system poles in a prespecified region of the left hand complex plane. This pole region, which can also be expressed as an LMI, was selected as a disk centered at $(-15 + j0)$ with radius $R = 15$ [12].

Finally, the minimization problem (10) is solved using LMI Toolbox. The set of LMIs was found feasible and a DynOF controller $K_f(s)$ of order 12 was computed, achieving $\gamma_\infty = 1.012$.

IV. Performance Analysis

Several simulations are carried out to derive the attitude responses due to tracking commands and wind disturbances for verifying the performance of the proposed full order controller $K_f(s)$. The robust performance of the single controller was demonstrated by applying it on nominal plant and the two extreme perturbed plants derived by setting $\Delta = +I$ and $\Delta = -I$. In all simulation results a stochastic wind signal of maximum aptitude 4m/s was employed [8].

In figure 4, the responses of the three closed-loop systems to separate step commands of 0.2 rad (10.45 deg) in ϕ_r, θ_r, ψ_r, respectively are shown. The blue color lines represent the responses of the nominal plant, while the green $(+\Delta)$ and red $(-\Delta)$ lines represent the responses of the plants perturbed by $\Delta = +I$ and $\Delta = -I$, respectively. For each figure the controlled output signal is drawn in solid line,while its rate is drawn in dashed line (- -). The rest output signals are drawn in dashed dot lines (-.).

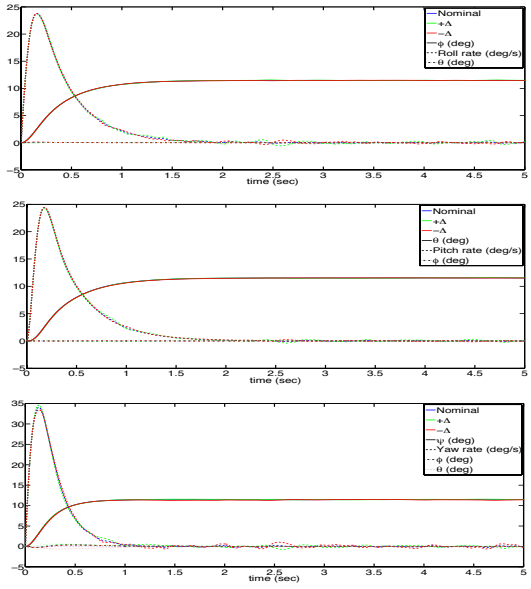

Fig. 4. Closed-loop response to ϕ_d command and wind disturbances

The controller achieves the specified settling and rise time, with near zero overshoots in all axis in the whole flight envelope. As it is expected the wind affects mostly the yaw channel but it is remaining within the desired bounds. Although not explicitly specified, our controller demonstrates a remarkable decoupling effect in the attitude dynamics. A summary of results is given in Table I.

Using the concept symmetric MIMO gain (GM), it is revealed that using the proposed single controller, the closed-loop systems can tolerate 25% gain variations at inputs

TABLE I

STEP RESPONSE CHARACTERISTICS

Axis		Nominal Plant	Perturbed Plant $(+\Delta)$	Perturbed Plant $(-\Delta)$
Roll	Overshoot	0.06%	0.06%	0.06%
	Settling/Rise	1.37s/ 0.75s	1.37s/ 0.75s	1.37s/ 0.75s
Pitch	Overshoot	0.59%	0.60%	0.59%
	Settling/Rise	1.37s/ 0.76s	1.40s/ 0.77s	1.40s/ 0.77s
Yaw	Overshoot	0.03%	0%	0%
	Settling/Rise	0.82s/ 0.45s	0.83s/ 0.45s	0.85s/ 0.45s

TABLE II

HANDLING QUALITIES RESULTS

HQ	Axis	Nominal Plant	Perturbed Plant$(+\Delta)$	Perturbed Plant$(-\Delta)$
(ω_{BW}, τ_p)	Roll	(3.06, 0.0063)	(3.25, 0.0057)	(2.91, 0.0069)
	Pitch	(1.8, 0.0371)	(1.82, 0.0372)	(2.91, 0.0370)
$\omega_{CF}(rad/s)$	Roll	3.92	3.94	3.90
	Pitch	4.45	4.51	4.37
$\frac{\Delta_{p(q,r)}}{\Delta_{\phi(\theta,\psi)}}(1/s)$	Roll	4.93	4.90	4.97
	Pitch	3.36	3.18	3.59
	Yaw	4.04	4.01	4.00

(actuators points), 20%gain variations at outputs (sensor points) and 126ms inputs time delays.

In order to assess our controller's compliance with the Level 1 requirements defined in ADS-33E, frequency domain responses are computed. We mainly focuses in three specifications: (i) the ratio of phase delay τ_p to bandwidth ω_{BW}, (ii) crossover frequency ω_{CF} and (iii) quickness ratio $\Delta_{p(q,r)}/\Delta_{\phi(\theta,\psi)}$. For a complete presentation of those terms see [10],[7],[1]. The results are shown in Table II.

V. HARDWARE IN THE LOOP SIMULATION

The final stage of any control design procedure is to be implemented and evaluated on a real platform. Nevertheless, hardware-in-the-loop (HIL) simulations are an essential intermediate step, especially in helicopter control design, to avoid disastrous effects due to malfunctions. Based on [17], among the various HIL schemes available, we choose scheme 6 (full simulation) in which the actuators, helicopter dynamics and sensors are simulated in a desktop PC and connected with the helicopter embedded system running all the necessary processes (control, navigation, sensor fusion, communication, e.t.c).

Our helicopter embedded system is a PC/104 having a dual-core Intel Atom N450@1.66GHz with Debian Squeeze Linux OS installed. The controller is implemented in the embedded system as a client module communicating with the multiplexor (server) as shown in Fig.5. The full nonlinear model (3) incorporating wind disturbances is simulated in MATLAB/SIMULINK® environment running on a desktop PC. Finally, the two systems are connected through an ethernet bus.

In order to verify the efficacy of the proposed attitude controller in "real" flight conditions, a total control structure with position tracking capabilities has to be constructed.

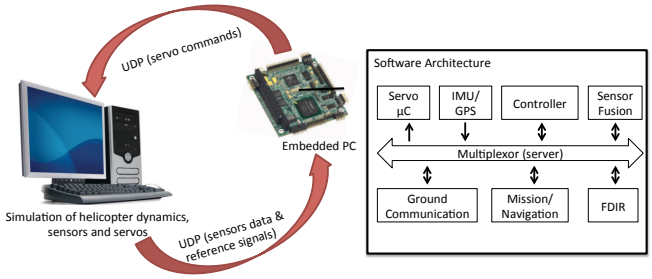

Fig. 5. HIL framework reprentation

For this purpose, a reduced order controller is designed combining of loop shaping and static output feedback control methods feeding back the total state vector of inner-closed subsystem (total system and $K_f(s)$ states) shown in Fig.2 [8]. Afterwards, the inverse transformation matrix (2) is used to transform the position error to body frame, while the inverse matrix of K_s^{δ} is used to transform the controller outputs (normalized inputs δ) to servo commands. Finally the total control structure is discretized (sampling time 10ms) and implemented in the embedded system.

To examine all possible couplings between the states of helicopter we use a multi-section trajectory inspired by real flights [1]. The helicopter starts from point (0,0,-20) in a hover condition at 20meters height and perform the below trajectories:

- *Section 1 (S_1) :* The helicopter moves forward accelerating to V_{air}^{nh} and decelerating back to hover condition at point (15.87,0,-20). (Overall Time: 10sec)
- *Section 2 (S_2) :* The helicopter makes a hover turn of 90 degrees. (Overall Time: 5sec)
- *Section 3 (S_3) :* The helicopter makes a vertical-longitudinal flight up to point (15.87,10,-30) (Overall Time: 10sec)
- *Section 4 (S_4) :* The helicopter makes a hover turn of 90 degrees. (Overall Time: 5sec)
- *Section 5 (S_5) :* The helicopter makes a slalom for 15m with maximum 2.5m side movement. (Overall Time: 15sec)
- *Section 6 (S_6) :* The helicopter makes a combination of forward flight and turn of 90 degrees up to point (-4.13,10,-30). (Overall Time: 5sec)
- *Section 7 (S_7) :* The helicopter makes a combination of decent flight and turn of 90 degrees up to point (-4.13,10,-20). (Overall Time: 10sec)
- *Section 8 (S_8) :* The helicopter hovers. (Overall Time: 5sec)

In all sections (exept S_1) the helicopter has fixed airspeed velocity up to V_{air}^{nh}. In the duration of flight a stochastic signal for the wind velocities is applied ($V_w^{max} = 4m/s$). The full response of helicopter is shown in Fig.6 and in more details in Fig.7.

Despite the fact that the full order attitude controller has 12 states and position controller has 3 states, the overall procedure from receiving the requested data and send back

the servo commands requires a remarkable average time of $61\mu s$ (max: $154\mu s$). Note that all the other processes (shown in Fig.5) are also running within the duration of HIL simulations.

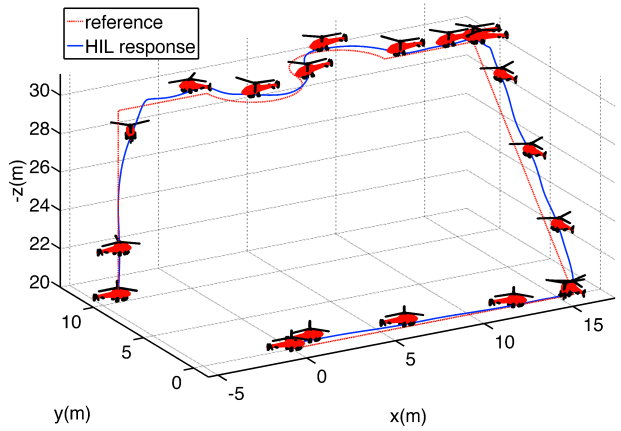

Fig. 6. Nonlinear helicopter model response with disturbances via HIL (3D)

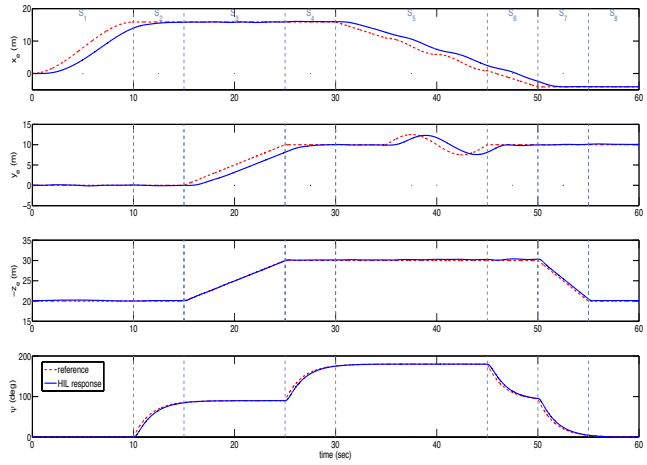

Fig. 7. Nonlinear helicopter model response (x_e, y_e, z_e, ψ) with disturbances via HIL (time scaled)

From the presented results, we can draw the conclusion that the proposed composite controller structure can successfully drive the helicopter along such a demanding trajectory and wind disturbances. Despite the fact that the position controller is designed to track step commands and reduce the wind disturbances, in all trajectory-sections the maximum error is less than 3 meters. Those errors mainly appear either when the helicopter tries to maintain its position while changing its orientation (S_2 ,S_4, S_6) or at the steep transition between sections. The constant error gap in S_3 and S_5 lies in the design of position controller as mentioned before.

VI. CONCLUSIONS

A systematic methodology for designing a robust mixed H_2/H_∞ attitude controller for a UAH in near hover flight was studied in this paper. As shown in the performance analysis, the proposed controller successfully passes all the demanding specifications guaranteeing stability, reference tracking, robustness and wind disturbance rejection through the whole near-hover flight envelope. HIL simulations shows two promising results - (i) combining the proposed approach with a simple position controller the helicopter can successfully track a demanding trajectory and (ii) a modern embedded system can easily handle full order multivariable controllers in a remarkable amount of time. This allows the possibility for designing more complex controllers. Our future work will focus on maximizing the range of flight envelope that can be handled by the proposed composite control structure and validating the efficiency of the controller in real flights using our under-construction platform.

REFERENCES

[1] G. Cai, B. Chen, and T. Lee, *Unmanned Rotorcraft Systems*, ser. Advances in Industrial Control. Springer, 2011.

[2] V. Gavrilets, B. Mettler, and E. Feron, "Nonlinear model for a small-size acrobatic helicopter," *AIAA guidance, navigation and control conference*, no. 2001-4333, 2001.

[3] L. Marconi and R. Naldi, "Aggressive control of helicopters in presence of parametric and dynamical uncertainties," *Mechatronics*, vol. 18, no. 7, pp. 381 – 389, 2008.

[4] I. A.Raptis, K. P. Valavanis, and W. Moreno, "A novel nonlinear backstepping controller design for helicopters using the rotation matrix," *IEEE Transactions on Control Systems Technology*, vol. 19, no. 2, pp. 465 –473, March 2011.

[5] G. Wanga, H. Shenga, T. Lub, D. Wanga, and F. Hua, "Development of an autonomous flight control system for small size unmanned helicopter," in *Robotics and Biomimetics, 2007. ROBIO 2007. IEEE International Conference on*, 2007, pp. 1804–1809.

[6] I. A. Raptis and K. P. Valavanis, *Linear and Nonlinear Control of Small-Scale Unmanned Helicopters*, ser. Intelligent Systems, Control and Automation: Science and Engineering Series. Springer, 2010.

[7] E. Prempain and I. Postlethwaite, "Static H_∞ loop shaping control of a fly-by-wire helicopter," *Automatica*, vol. 41, pp. 1517–1528, 2005.

[8] J. Gadewadikar, F. L. Lewis, K. Subbarao, K. Peng, and B. M. Chen, "H_∞ static output-feedback control for rotorcraft," *Journal of Intelligent and Robotic Systems*, pp. 629–646, 2009.

[9] H.-q. Wang, A. Mian, D.-b. Wang, and H.-b. Duan, "Robust multi-mode flight control design for an unmanned helicopter based on multi-loop structure," *International Journal of Control, Automation and Systems*, vol. 7, pp. 723–730, 2009, 10.1007/s12555-009-0504-1.

[10] ADS-33D-PRF, "Aeronautical design standard performance specification handling qualities requirements for military rotorcraft," U.S. Army Aviation and Troop Command, Tech. Rep., 1996.

[11] S. Skogestad and I. Postlethwaite, *Multivariable Feedback Control: Analysis and Design*. New York, NY, USA: John Wiley & Sons, Inc., 1996.

[12] C. Scherer, P. Gahinet, and M. Chilali, "Multiobjective output-feedback control via lmi optimization," *IEEE Transactions on Automatic Control*, vol. 42, no. 7, pp. 896 –911, July 1997.

[13] P. C. Pellanda, P. Apkarian, and H. D. Tuan, "Missile autopilot design via a multi-channel lft/lpv control method," *Int. Journal of Robust and Nonlinear Control*, vol. 12, pp. 1–20, 2002.

[14] D.-Y. Won, M.-J. Tahk, and Y.-H. Kim, "Three-axis autopilot design for a high angle-of-attack missile using mixed H_2/H_∞ control," *Int. Journal of Aeronautical & Space Sci.*, vol. 11, no. 2, pp. 131–135, June 2010.

[15] O. D. Jaulin L., M. Kieffer and E. Walter, *Applied Interval Analysis with Examples in Parameter and State Estimation, Robust Control and Robotics*. Springer-Verlag, 2001, no. ISBN: 1-85233-219-0.

[16] P. Apkarian, G. Becker, P. Gahinet, and H. Kajiwara, "LMI techniques in control engineering from theory to practice," in *Workshop Notes - IEEE Conference on Decision and Control*, Kobe, Japan, Dec. 1996.

[17] R. Isermann, J. Schaffnit, and S. Sinsel, "Hardware-in-the-loop simulation for the design and testing of engine-control systems," *Control Engineering Practice*, vol. 7, no. 5, pp. 643 – 653, 1999.